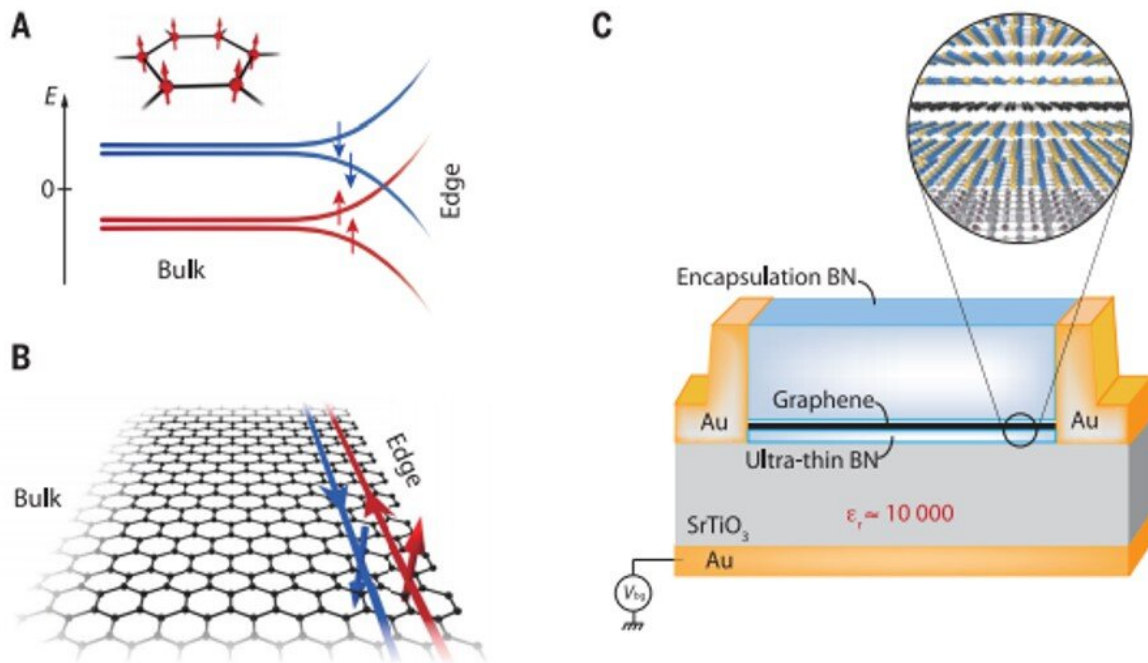


Helical quantum Hall phase in graphene on strontium titanate

February 28 2020, by Thamarasee Jeewandara



Spin-polarized ferromagnetic phase in graphene on high- k dielectric. (A) In the ferromagnetic phase of charge-neutral graphene, the broken-symmetry state of the half-filled zeroth Landau level is spin polarized and occupies both sublattices of the honeycomb lattice, as shown in the inset. The edge dispersion results from linear combinations of the bulk isospin states, which disperse as electron-like and hole-like branches, yielding a pair of counter-propagative, spin-filtered helical edge channels at charge neutrality. Red and blue arrows represent the spin polarization of the sublevels. (B) Schematic of a graphene lattice with helical edge channels propagating on the crystallographic armchair edge. (C) Schematic of the hBN-encapsulated graphene device placed on a SrTiO₃ substrate that serves both as a high-dielectric constant environment and a back-gate dielectric.

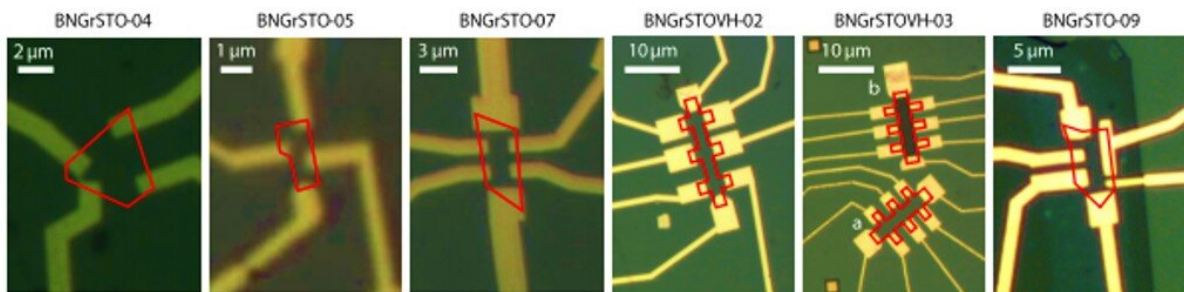
Owing to the considerable dielectric constant ($\epsilon_r \sim 10,000$) of the SrTiO₃ substrate at low temperature and the ultrathin hBN spacer (2 to 5 nm thick), Coulomb interaction in the graphene plane is substantially screened, resulting in a modification of the quantum Hall ground state at charge neutrality and the emergence of the ferromagnetic phase with helical edge transport. The magnified view shows atomic layers of the hBN-encapsulated graphene van der Waals assembly and the surface atomic structure of SrTiO₃. Credit: *Science*, doi: 10.1126/science.aax8201

Materials that exhibit topological phases can be classified by their dimensionality, symmetries and topological invariants to form conductive-edge states with [peculiar transport](#) and spin properties. For example, [the quantum Hall effect](#) can arise in two-dimensional (2-D) electron systems subjected to a perpendicular magnetic field. When distinct characteristics of quantum Hall systems are compared with [time-reversal symmetric](#) (entropy conserved) [topological insulators](#) (TIs), they appear to rely on [Coulomb interactions](#) between electrons to induce a wealth of strongly correlated, topologically or symmetry-projected phases in a [variety of experimental systems](#).

In a new report now on *Science*, Louis Veyrat and a research team in materials science, [quantum optics](#) and optoelectronics in France, China and Japan tuned the ground state of the graphene zeroth [Landau level](#) i.e. orbitals occupied by charged particles with discrete energy values. Using suitable screening of the Coulomb interaction with the high [dielectric constant](#) of a [strontium titanate](#) (SrTiO₃) substrate, they observed robust helical edge transport at magnetic fields as low as 1 Tesla, withstanding temperatures of up to 110 kelvin across micron-long distances. These versatile graphene platforms will have applications in [spintronics](#) and [topological quantum computation](#).

Topological insulators (TIs), i.e., a material that behaves as an insulator

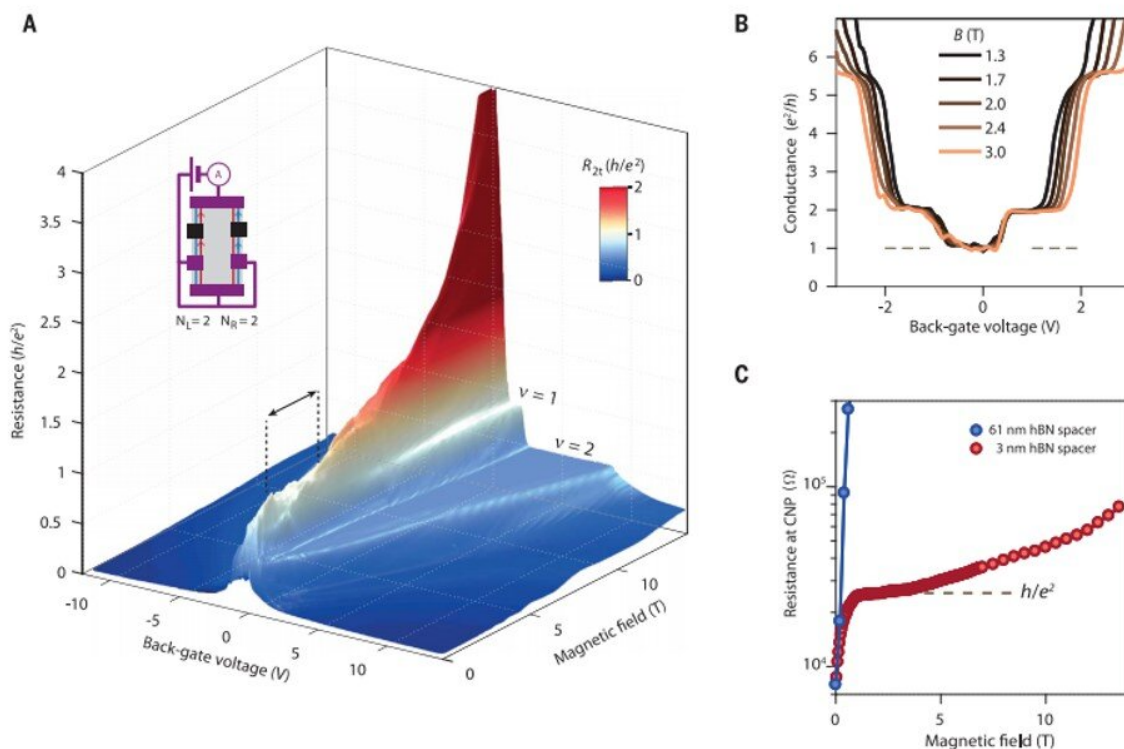
in its interior but retains a conducting surface state, with zero [Chern number](#) have emerged as quantum Hall [topological insulators](#) (QHTIs) arising from many-body interacting Landau levels. They can be pictured as two independent copies of quantum Hall systems with opposite chirality, but the experimental system is at odds with the described scenario, where a strong insulating state is observed on increasing the perpendicular [magnetic field](#) in charge-neutral, high-mobility graphene devices.



Graphene devices. Optical pictures of diverse samples. The red lines underline the edges of the hBN-encapsulated graphene flakes. Credit: Science, doi: 10.1126/science.aax8201

The experimental formation of the ferromagnetic (F) phase (F-phase) in graphene is therefore potentially hindered by such lattice-scale electron-electron and [electron-phonon](#) interactions. To overcome this, scientists had previously applied a very strong in-plane magnetic field component higher than 30 Tesla to surpass [anisotropic interactions](#), allowing the F-phase [to experimentally emerge](#) in graphene. In another strategy they used [graphene bilayers](#) hosting two different quantum Hall states of opposite charge-carrier types, but they suffered from an impractically strong and tilted magnetic field or complexity of materials assembly. As

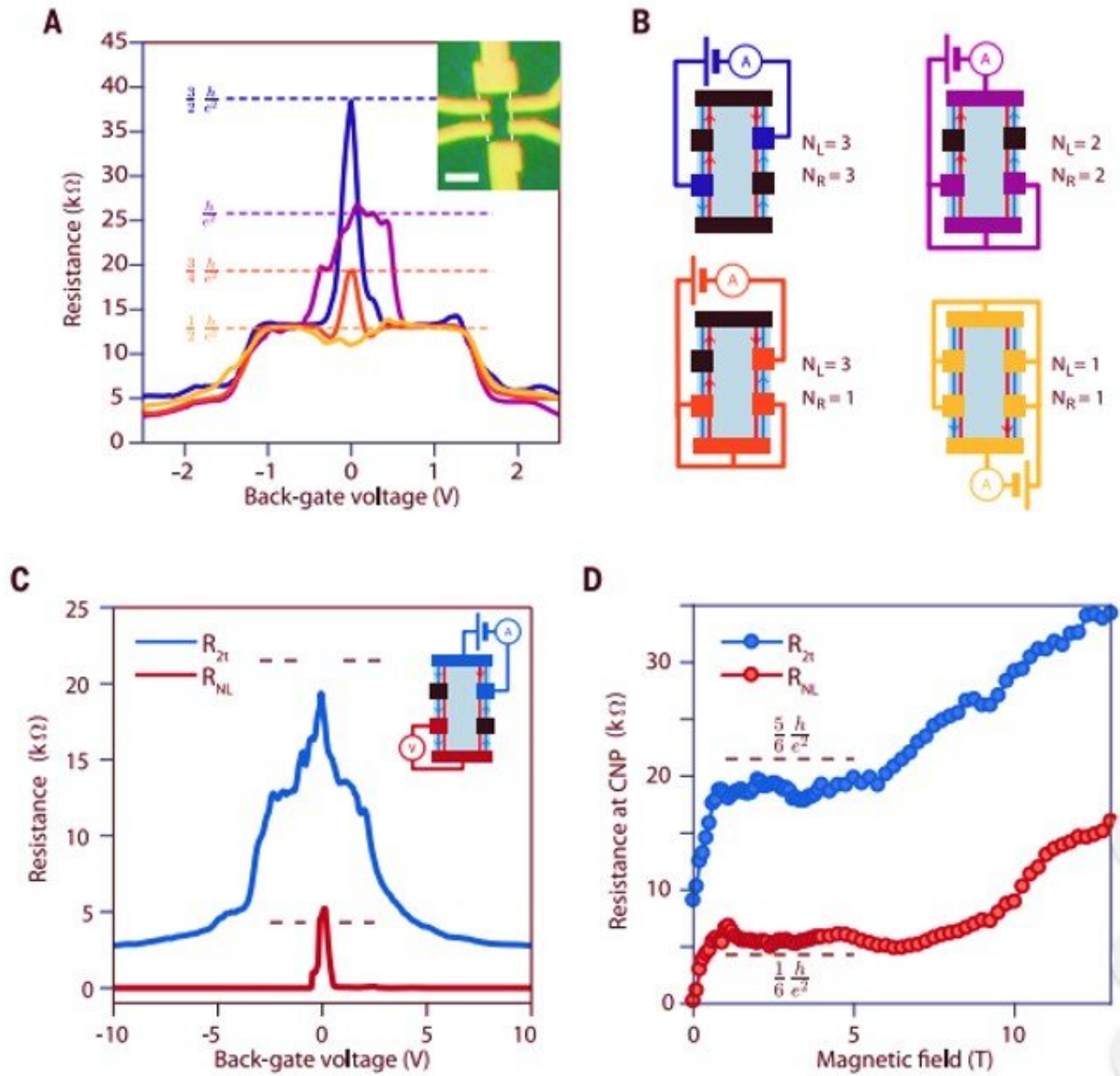
a result, in this work Veyrat et al. used a different approach to induce the F-phase in monolayer graphene. Instead of boosting the [Zeeman energy](#) or [Zeeman effect](#) i.e. splitting a spectral line using a magnetic field to overcome anisotropic interactions, they modified the lattice-scale interactions relative to Coulomb interactions to restore the dominant role of the spin-polarizing terms and induce the F-phase.



Low-magnetic field quantum spin Hall effect. (A) Two-terminal resistance R_{2t} in units of h/e^2 of sample BNGrSTO-07 versus magnetic field and back-gate voltage measured at 4 K. In addition to standard quantum Hall plateaus at filling fractions $n = 1$ and 2 , the resistance exhibits an anomalous plateau around the charge neutrality point between $B = 1.5$ and 4 T, delimited by the black dashed lines and the double-headed arrow, which signals the regime of the QSH effect in this sample. The value of the resistance at this plateau is h/e^2 and is color coded white. The inset schematic indicates the contact configuration. Black contacts are floating. The red and blue arrows on the helical edge channels

indicate the direction of the current between contacts, and A indicates the ampere meter. (B) Two-terminal conductance $G_{2t} = 1/R_{2t}$ in units of e^2/h versus back-gate voltage extracted from (A) at different magnetic fields. The first conductance plateaus of the quantum Hall effect at $2e^2/h$ and $6e^2/h$ are well defined. The QSH plateau of conductance e^2/h clearly emerges at charge neutrality around $V_{bg} = 0$ V. (C) Resistance at the charge neutrality point (CNP) versus magnetic field for sample BNGrSTO-07 (red dots) extracted from (A) and sample BNGrSTO-09 (blue dots). The latter sample has a thick hBN spacer and exhibits a strong positive magnetoresistance at low magnetic field diverging toward insulation; the sample with the thin hBN spacer (BNGrSTO-07) shows a QSH plateau that persists up to ~ 4 T, followed by a resistance increase at higher magnetic field. W, ohms. Credit: Science, doi: 10.1126/science.aax8201

For this, they used quantum paraelectric strontium titanate (SrTiO_3), known to exhibit a large static dielectric constant ($D \approx 10^4$) at [low temperatures](#). The setup eventually modified the ground state of graphene at charge neutrality. Veyrat et al. accomplished this by engineering [high-mobility graphene](#) heterostructures based on [hexagonal boron nitride](#) (hBN) encapsulation and readily observed the emergence of the F-phase in a screened configuration. By changing the source of electrons and drain (flow of electrons) contacts in the setup, and the number of helical edge sections, they observed [helical edge transport](#). Veyrat et al. also observed simultaneous measurements of two-terminal resistances and non-local resistance while keeping the same source and drain current-injection contacts to demonstrate current flow on the edges of the sample.

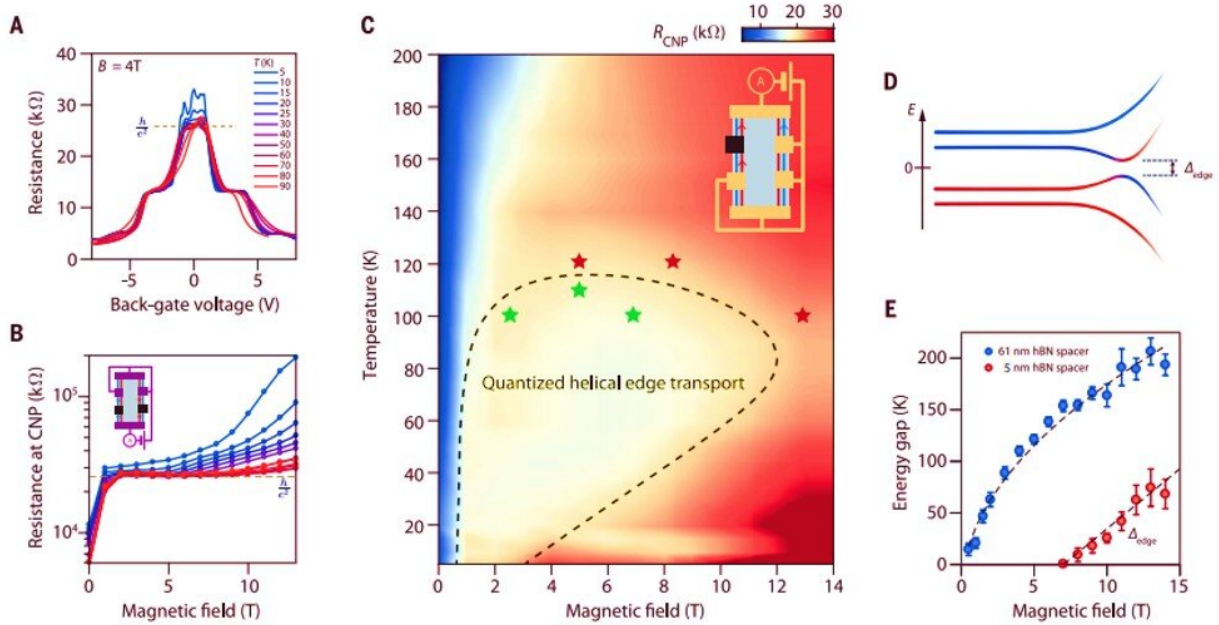


Nonlocal helical edge transport. (A) Two-terminal resistance versus back-gate voltage measured at 2.5 T and 4 K for different contact configurations schematized in (B). The inset shows an optical picture of the measured sample BNGrSTO-07. The scale bar is 4 μm . Each contact configuration yields a resistance at charge neutrality reaching the expected values for helical edge transport, which are indicated with the horizontal dashed lines. (B) Schematics of the measurement configurations. Black contacts are floating. The red and blue arrows on the helical edge channels indicate the direction of the current between contacts. (C) Two-terminal resistance, R_{2t} , in blue and nonlocal, four-terminal

resistance, RNL, in red versus back-gate voltage in the contact configuration shown in the inset schematic. In the schematic, V indicates the voltmeter. (D) Resistance at the CNP, $V_{bg} = 0$ V, in the same contact configuration as in (C) versus magnetic field. The helical plateau is observed for both two- and four-terminal resistances between 1 T and about 6 T. Credit: Science, doi: 10.1126/science.aax8201

To investigate robustness of helical edge transport, the team conducted systematic studies of its temperature and magnetic field dependence. The SrTiO_3 dielectric constant remained high enough up to 200 K, and the dielectric screening remained virtually unaffected. To understand the limit of quantized helical edge transport, the team measured different contact configurations at several magnetic field and temperature values to show that quantized helical edge transport could withstand very high temperatures of up to 110 K.

The team then demonstrated the key role of the SrTiO_3 dielectric substrate during F-phase establishment. Due to substantially reduced electron-electron interactions in a high-dielectric constant measurement, the F-phase emerged as a ground state in the control experiments. Veyrat et al. further investigated the screening effects and short-range lattice-scale contributions of the Coulomb and electron-phonon interactions to determine the energetically favorable ground state. The observed mechanisms will open exciting new perspectives. For instance, the Coulomb energy scale could be enhanced by increasing the magnetic field to induce a topological quantum phase transition from the QHTI (quantum Hall topological insulators) ferromagnetic phase to an insulating, trivial quantum Hall ground state—a type of transition [hitherto little addressed](#).



Phase diagram of the helical edge transport. (A) Two-terminal resistance of sample BNGrSTO-07 versus back-gate voltage measured at various temperatures and a magnetic field of 4 T. The back-gate voltage is renormalized to compensate the temperature-dependence of the substrate dielectric constant. (B) Two-terminal resistance at the CNP for the same data as in (A). The inset shows the contact configuration used in (A) and (B). (C) Two-terminal resistance at the CNP versus magnetic field and temperature for a different contact configuration shown in the inset. The resistance shows a plateau at the value expected for helical edge transport ($2.3 h e^2$, color coded light yellow) over a large range of temperatures and magnetic fields, that is, up to $T = 110$ K at $B = 5$ T. The stars indicate the parameters at which helical edge transport has been checked by measuring different contact configurations. (Green stars indicate quantized helical edge transport, and red stars indicate deviation to quantization at the CNP.) The dashed curve is a guide for the eye showing the approximate limits of the quantized helical edge transport of the F phase. (D) Schematic of the edge dispersion of the zeroth Landau level broken-symmetry states showing the opening of a gap at the edge. (E) Activation energy at the charge neutrality point versus magnetic field measured in samples BNGrSTOVH-02 (red dots) and BNGrSTO-09 (blue dots), which have hBN spacers of 5 and 61 nm, respectively. The dashed lines are a linear fit for BNGrSTOVH-02 and a fit of the dependence for BNGrSTO-09. The prefactor $\alpha = 64$ $KT^{-1/2}$ corresponds to a

disorder-free gap, and the intercept describes the disorder-broadening of the Landau levels, which is consistent with the sample mobility. Credit: Science, doi: 10.1126/science.aax8201

In this way, Louis Veyrat and colleagues demonstrated the ferromagnetic (F) phase in screened graphene. The setup emerged at low magnetic fields as a prototypical interaction-induced topological phase with robust helical edge transport. The edge excitations were tunable with magnetic fields to study zero-energy modes in superconductivity-[proximitized](#) architectures. The method of substrate-screening engineering was tunable due to the thickness of the hBN spacer used in the study, the team therefore expect the ground states and optoelectronic properties of other correlated 2-D systems to be as strongly influenced by their dielectric environment.

More information: Louis Veyrat et al. Helical quantum Hall phase in graphene on SrTiO₃, *Science* (2020). [DOI: 10.1126/science.aax8201](https://doi.org/10.1126/science.aax8201)

Javier D. Sanchez-Yamagishi et al. Helical edge states and fractional quantum Hall effect in a graphene electron–hole bilayer, *Nature Nanotechnology* (2016). [DOI: 10.1038/nnano.2016.214](https://doi.org/10.1038/nnano.2016.214)

A. F. Young et al. Tunable symmetry breaking and helical edge transport in a graphene quantum spin Hall state, *Nature* (2013). [DOI: 10.1038/nature12800](https://doi.org/10.1038/nature12800)

© 2020 Science X Network

Citation: Helical quantum Hall phase in graphene on strontium titanate (2020, February 28) retrieved 19 April 2024 from

<https://phys.org/news/2020-02-helical-quantum-hall-phase-graphene.html>

This document is subject to copyright. Apart from any fair dealing for the purpose of private study or research, no part may be reproduced without the written permission. The content is provided for information purposes only.